Supplementary Material

Supplementary Material Part I:

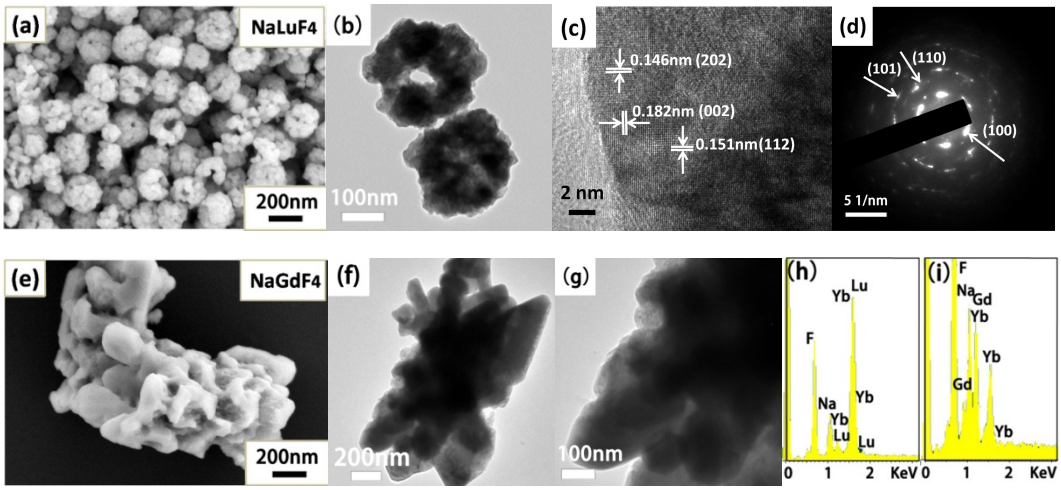

Figure S1 $NaLuF_4$:Yb^{3+}, Er^{3+} hollow flower-like assemblies: SEM (a), TEM (b), HRTEM (c), SAED (d) and EDS (h). $NaGdF_4$:Yb^{3+}, Er^{3+} porous rods: SEM (e), TEM (f), local magnification (g) and EDS (i). As for the (002) crystal plane, the measured lattice distance is 0.146 nm (theoretical value is 0.143 nm).

With the burst of $NaLuF_4$ precursors, it may produce plenty of 'explosive fragments' and 'gas nucleus'. With the time extension, these small freak nanoparticles (40-60nm) got together, surrounded by gas nucleus and fused to $NaLuF_4$:Yb^{3+},Er^{3+} hollow flower-like assemblies (diameter in 200-250nm, Fig. S1a-b). The inner hollow structure in these uncompleted assemblies was also clearly observed. The measured lattice distance (Fig. S1c) is a slightly bigger than theoretical value due to the crystal lattice distortion would expand lattice constant of host materials when the bigger ionic radius Yb^{3+} or Er^{3+} doped into $NaLuF_4$ substrates. As for the XRD patterns of doped $NaLuF_4$ upconversion nanocrystals, they always had 1-5 degree shifts towards small angle direction, further identifying the crystal lattice distortion process. The poly-crystalline nature of nanocrystals was confirmed by SAED rings (Fig. S1d). Different with $NaLuF_4$ nanocrystals, the explosion of $NaGdF_4$ didn't entirely destroy rod-like structure but only destroy the outer materials to produce porous structure (Fig. S1e-g). The elementary composition of $NaLuF_4$:Yb^{3+}, Er^{3+} and $NaGdF_4$:Yb^{3+}, Er^{3+} were also analyzed by the EDS analysis (Fig. S1h-i).

Supplementary Material Part II:

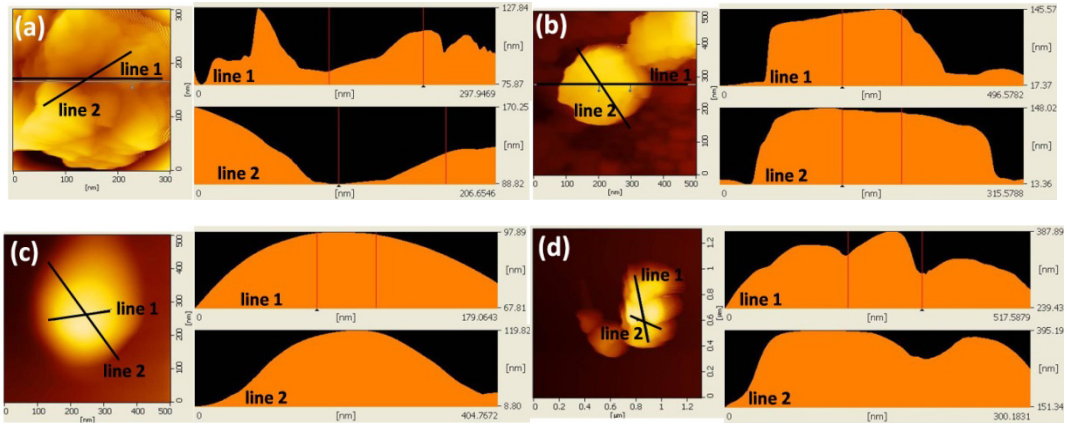

Figure S2 AFM images of products at different reaction time (a) 0h, (b) 1h, (c) 3h of $NaLuF_4$ flower-like assemblies and AFM image (d) is corresponding to $NaGdF_4$ porous rods in 12h.

To further verify the 'From rough to smooth surface' stage of $NaLuF_4$ flower-like assemblies, we apply AFM techniques (atomic force microscopy, Fig. S2) as another characteristic means of 'stage I' changes. As the hydrothermal reaction, surfaces of nanospheres range from rough to smooth in hydrothermal system about 3 h. The average roughness (Ra) value changes from 9.855nm (0h) to 6.716nm (1h), and when hydrothermal time reach about 3h, the Ra is 1.457nm. From AFM images, we observe that there are some larger hollow cavities in the substrates microrods and the shape of hollow cavities is irregular. For the two line profiles, the size of cavities are about 60-80nm, and the maximum depth of pore defects is about 80 nm. These AFM images can match well with our SEM images.

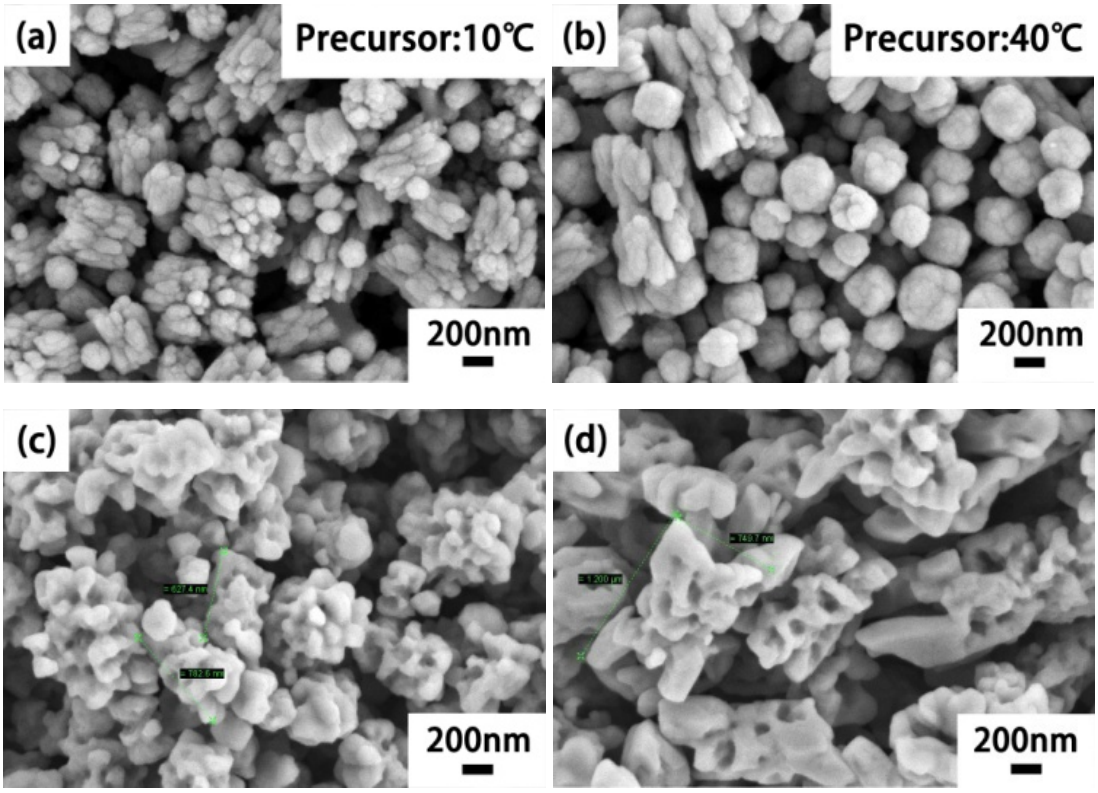

Figure S3 Precursor of $NaGdF_4$ prepared in 10 ^oC (a) and 40 ^oC (b). SEM images (c) and (d) are the products of 'precursor 10 ^oC' and 'precursor 40 ^oC' in 230 ^oC for 12h respectively.

In the hydrothermal system, we found the temperature of preparing precursors may both have an effect on the morphologies of precursors and final products (Fig. S3). The elevated temperature will be helpful to assemble bigger precursors, because the elevated temperature may lead to higher surface activity of nanocrystals which is more conducive to promote the assmeblies among nanocrystals. Comparative analysis of SEM (c) and (d), we found that the porous $NaGdF_4$ rods may have bigger size and more clear outline appearance in the situation of 'precursor 40 ^oC'. This reminds us that the temperature is an important element in the process of preparing precursors. This phenomenon also gives us a new enlightenment that we can change the temperature of preparing precursors to modulate the final morphology and size of products.

Supplementary Material Part III:

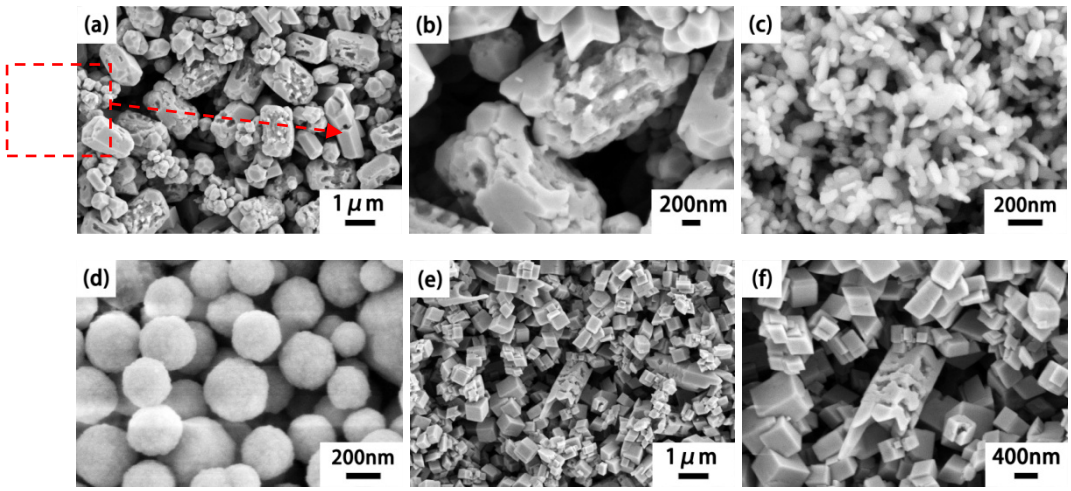

Figure S4 The products of decreasing the proportion of DDBAC/ Gd to 0.5 (a) and its local manigication (b). Only use DDBAC as additives (c). only use GA as additives to get precursors (d), products (e) and their local magnification (f).

As control groups with porous $NaGdF_4$ rods, we decreased the additive amount of DDBAC, and then prepared bigger porous columnar structure (Fig. S4). Using DDBAC as only one additive (c), the smooth fusiform $NaGdF_4$ nanocrystals can be prepared with the size about 100-150nm. Comparing with $NaLuF_4$ nanoparticles with only DDBAC, we found that the $NaGdF_4$ tended to form the approximate rod structure. It may be caused by the special structure of outer electrons of Gd^{3+} ions. We also tried to use single GA to get rough spherical precursors and corresponding prismatic products of $NaGdF_4$. These experiments also verify the function of DDBAC and GA which can act as morphology, size control agent and 'explosive powder'.

Supplementary Material Part IV:

Table.1 Data are from SEM observations (Figure S5) as follows.

Proportion / Temperature	F: Lu=4	F: Lu=8	F: Lu=12
Precursor	1. Loose and rough particles assembled by small precursor particles. 2 . About 100-250nm	The same morphology and size distribution with precursor at 'F: Lu=4'.	The same morphology and size distribution with precursor at 'F: Lu=4'.

230 °C	1. Rough particles with porous structure prepared by 'explosion' method. 2. About 50-200nm	1. Spindly hexagonal columnar structure with smooth surface. 2. L: D≈ 14.2	1. Hexagonal columnar structure with smooth surface. 2. L: D≈ 3.46
240 °C	1. Bigger and short micro-columnar structure with small particles on the surface. 2. The size of small particles: 40-50nm.	1. Spindly hexagonal columnar structure with end recess. 2. L: D≈ 6.4	1. Hexagonal columnar structure with end recess. 2. L: D≈ 4.47
250 °C	1. Short micro-columnar structure with small particles on the surface. 2. The size of small particles: 40-50nm.	1. Spindly hexagonal columnar structure with end recess. 2. L: D≈ 27.5	1. Hexagonal columnar structure with end recess. 2. L: D≈ 4.45

(L: D represents the length-diameter ratio.)

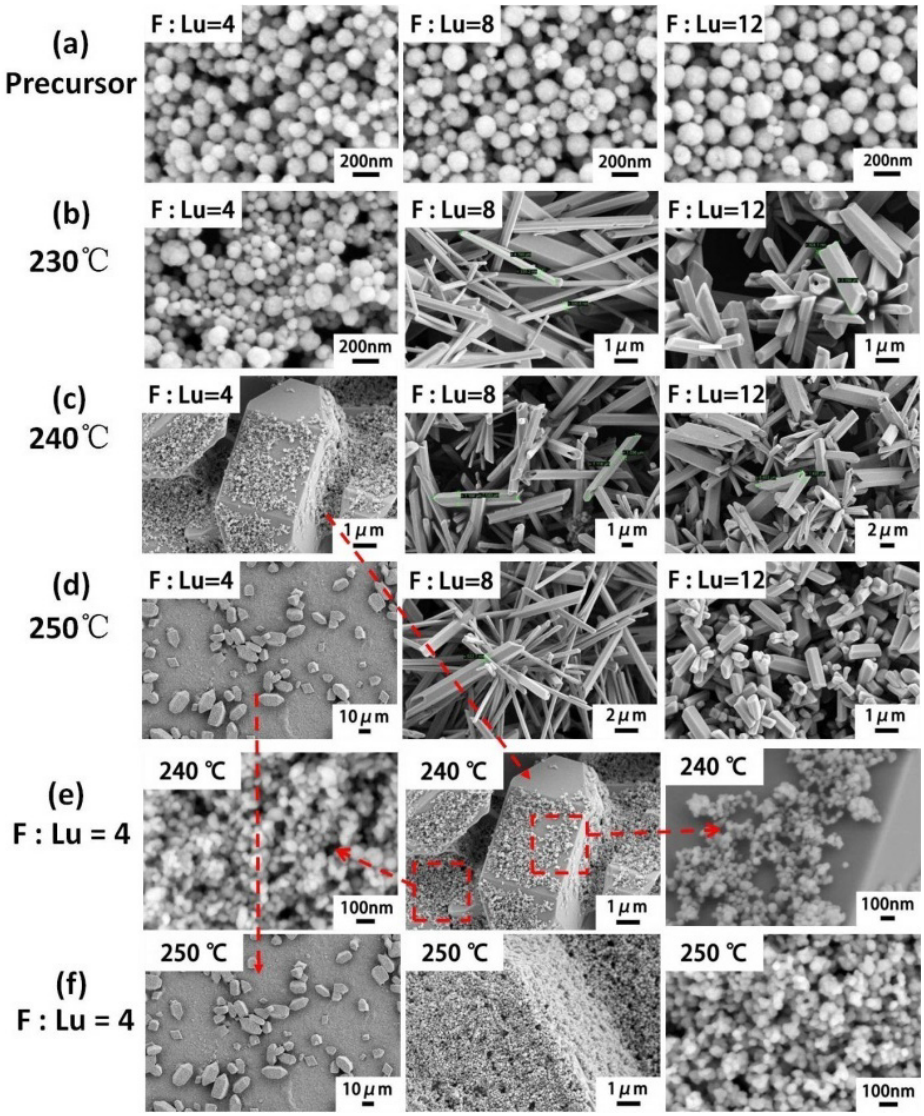

Figure S5 SEM images of $NaLuF_4$ samples at different proportions of F/Lu and hydrothermal temperature conditions at 12 hours with only GA addition (a-f).

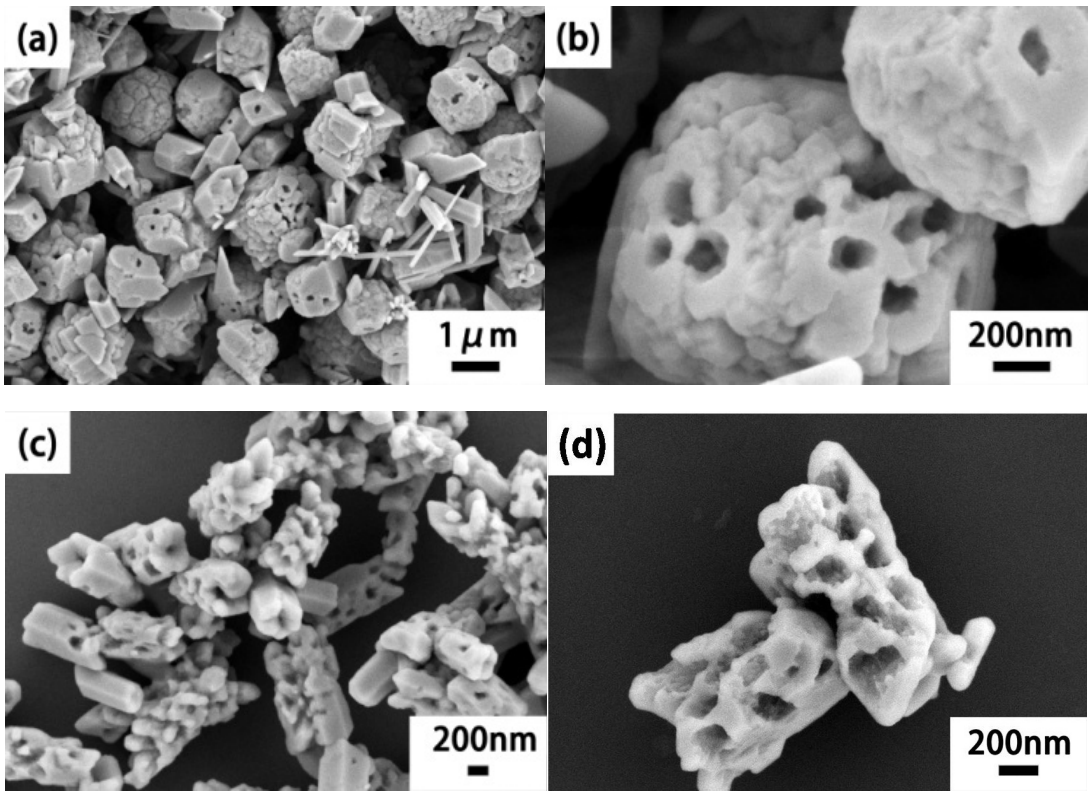

Figure S6 The influence to final products at different proportions of F/Gd: SEM (a) the products of F/Gd =6 and (b) its local magnification. SEM (c) the products of F/Gd =12 and (d) its local magnification.

To further verify the universal function of fluorine ions on final product morphologies, we choose two proportions of 'F/Gd =6' and 'F/Gd =12' to prepare two morphological products: short porous columnar (L: D≈ 0.5) and approximately porous rod structures (L: D≈ 2.5). Owing to the discrepancies of absorption capability on different crystal faces for excessive fluorine ions, the higher proportion of F/Gd increase the length-diameter ratio of $NaGdF_4$ (Figure S6).

Supplementary Material Part V:

We construct these models and mechanical simulations based on the 'Generalized Hooke law'.

$$\sigma_x = C_{11}\varepsilon_x + C_{12}\varepsilon_y + C_{13}\varepsilon_z + C_{14}\gamma_{xy} + C_{15}\gamma_{yz} + C_{16}\gamma_{zx}$$

$$\sigma_y = C_{21}\varepsilon_x + C_{22}\varepsilon_y + C_{23}\varepsilon_z + C_{24}\gamma_{xy} + C_{25}\gamma_{yz} + C_{26}\gamma_{zx}$$

$$\sigma_z = C_{31}\varepsilon_x + C_{32}\varepsilon_y + C_{33}\varepsilon_z + C_{34}\gamma_{xy} + C_{35}\gamma_{yz} + C_{36}\gamma_{zx}$$

$$\tau_{xy} = C_{41}\varepsilon_x + C_{42}\varepsilon_y + C_{43}\varepsilon_z + C_{44}\gamma_{xy} + C_{45}\gamma_{yz} + C_{46}\gamma_{zx}$$

$$\tau_{yz} = C_{51}\varepsilon_x + C_{52}\varepsilon_y + C_{53}\varepsilon_z + C_{54}\gamma_{xy} + C_{55}\gamma_{yz} + C_{56}\gamma_{zx}$$

$$\tau_{zx} = C_{61}\varepsilon_x + C_{62}\varepsilon_y + C_{63}\varepsilon_z + C_{64}\gamma_{xy} + C_{65}\gamma_{yz} + C_{66}\gamma_{zx}$$

In this formula, C_{ij} (i,j=1,2……6) is 'stiffness constant', representing the proportion coefficient of the stress component and strain component.

Through simple operations and processing, we transform above formula into 'flexibility constant' expression which is more intuitive expression of 'elastic coefficient', and then we make some simplified processing to reduce the number of independent elastic constants.

$$S = \begin{bmatrix} S_{11} & S_{12} & S_{12} & 0 & 0 & 0 \\ 0 & S_{11} & S_{12} & 0 & 0 & 0 \\ 0 & 0 & S_{11} & 0 & 0 & 0 \\ 0 & 0 & 0 & 2(S_{11}-S_{12}) & 0 & 0 \\ 0 & 0 & 0 & 0 & 2(S_{11}-S_{12}) & 0 \\ 0 & 0 & 0 & 0 & 0 & 2(S_{11}-S_{12}) \end{bmatrix}$$

In most situations for metal or ceramic materials, we can regard them as isotropic body, S_{11} and S_{12} are two independent flexibility constants.

$$E = \frac{1}{S_{11}}$$

$$v = \frac{S_{12}}{S_{11}}$$

$$G = \frac{1}{2(S_{11}-S_{12})}$$

Combining with these basic mechanics parameters, we can infer the base formulas for simulations.

$$\varepsilon_x = \frac{1}{E}[\sigma_x - v(\sigma_y + \sigma_z)]$$

$$\varepsilon_y = \frac{1}{E}[\sigma_y - v(\sigma_z + \sigma_x)]$$

$$\varepsilon_z = \frac{1}{E}[\sigma_z - v(\sigma_x + \sigma_y)]$$

$$\gamma_{xy} = \frac{1}{G}\tau_{xy}$$

$$\gamma_{yz} = \frac{1}{G}\tau_{yz}$$

$$\gamma_{zx} = \frac{1}{G}\tau_{zx}$$

Parameters for the yield force models:

Big sphere: (R: radius); Circular column: (R: radius, H: high); Hole: (r: radius); 'D': the distance between hole and model surface; 'd': the distance between two holes.

Their values are expressed with the 'unit length' as a reference. These models materials and the load for every hole all maintains the same, so that we can compare the result with each other. To simulate the explosive situation reasonably, we use some 'holes' to represent the original explosive places, such as dislocation defects, micro-tunnels and some other inside loose structures.

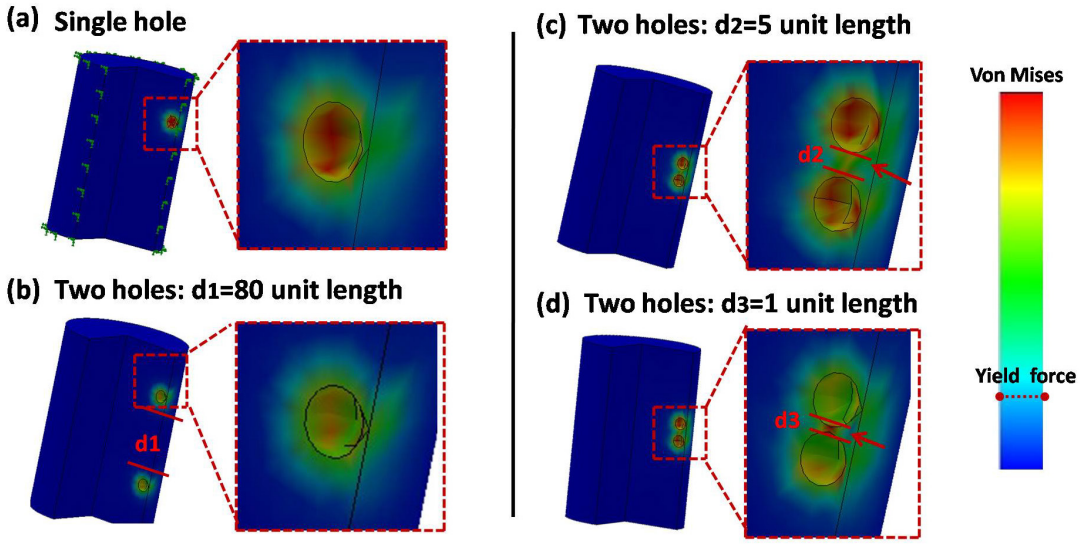

Figure S7 'Blob and oriented blast': the stress distribution for single hole (a), two holes with distant distance (b), the distance about 5 unit length (c) and 1 unit length (d).

Observing from SEM of porous rods, we find that there are small holes and bigger holes. And then evaluating from mechanical simulations (a) to (d), there are two ways to produce these two kinds of porous size distribution. For the situation of 'distant two holes', they blast separately to produce small holes on the lateral surface of rods just like the explosive way of 'single hole'. With the distance shortening between two holes, the color of middle zone changes from 'blue' to 'orangered' gradually, which means that material in middle zone is easier to be damaged under so big stress distribution. So the two holes prefer to link together at first, and then blast together to form bigger holes.

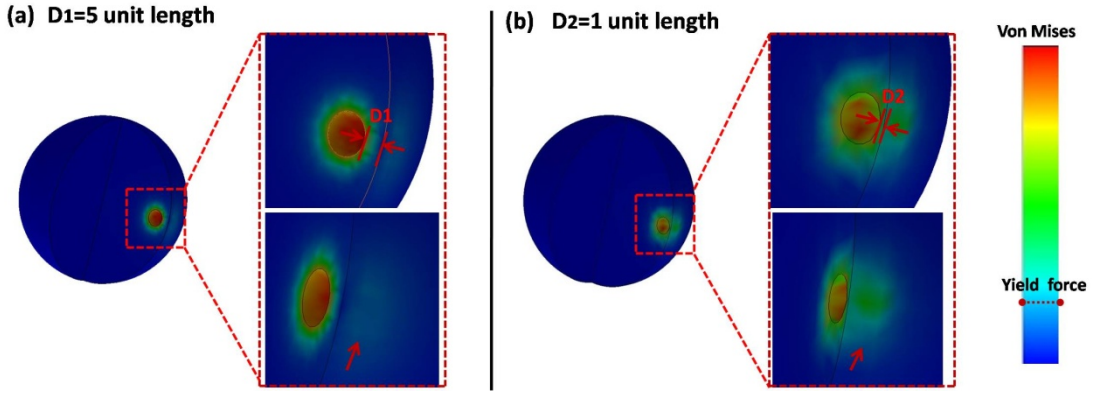

Figure S8 'Superficial zone blast': the stress distribution for different distance between hole and outside spherical surface.

This style is a mild explosion to continuously produce superficial porous structure just like the surface of 'moon'. With the distance between hole and outside surface reducing from 5 to 1, 'green area' on the surface becomes larger, which means that the hole with shorter distance prefers to produce porous structure on the surface. And then we found that color changed area is generally larger than original hole, which can verify the original explosive place can exist a very tiny area, such as dislocation defects, micro-tunnels and some other inside loose structures.